ANS NCSD 2013 - Criticality Safety in the Modern Era: Raising the Bar
Wilmington, NC, September 29 –October 3, 2013, on CD-ROM, American Nuclear Society, LaGrange Park, IL (2013)

ANALYSIS OF MEASURED DATA FROM EXPERIMENTS 2 AND 3 OF THE 2010 CRITICALITY ACCIDENT ALARM SYSTEM BENCHMARK AT THE CEA VALDUC SILENE FACILITY

T. M. Miller, M. E. Dunn, J. C. Wagner, and K. L. McMahan
Oak Ridge National Laboratory
P. O. Box 2008, MS-6170
Oak Ridge, Tennessee, 37831, USA
millertm@ornl.gov, dunnme@ornl.gov, wagnerjc@ornl.gov, and mcmahankl@ornl.gov

N. Authier, X. Jacquet, G. Rousseau, H. Wolff, J. Piot, L. Savanier, and N. Baclet
Commissariat à l'Énergie Atomique et aux Énergies Alternatives —Centre de Valduc
Service de Recherche en Neutronique et Criticité
21120 Is sur Tille, France
nicolas.authier@cea.fr, xavier.jacquet@cea.fr, guillaume.rousseau@cea.fr, herve.wolff@cea.fr, jerome.piot@cea.fr, laurence.savanier@cea.fr, and nathalie.baclet@cea.fr

Y.-K. Lee, V. Masse[1], J.-C. Trama, E. Gagnier, S. Naury, and P. Blanc-Tranchant
Commissariat à l'Énergie Atomique et aux Énergies Alternatives —Centre de Saclay
DEN/DANS/DM2S/SERMA
91191 Gif sur Yvette Cedex, France
yi-kang.lee@cea.fr, veronique.masse@cea.fr, jean-christophe.trama@cea.fr, emmanuel.gagnier@cea;fr, sylvie.naury@cea.fr, and patrick.blanc-tranchant@cea.fr

R. HUNTER
Babcock International Group
2100 Daresbury Park
Daresbury, Warrington, WA4 4HS, England
richard.hunter@babcockinternational.com

S. KIM and G. M. DULIK
Lawrence Livermore National Laboratory
P. O. Box 808
Livermore, California, 94551, USA
kim53@llnl.gov and dulik1@llnl.gov

K. H. REYNOLDS
Y-12 National Security Complex
P. O. Box 2009
Oak Ridge, Tennessee, 37831, USA
reynoldskh2@y12.doe.gov

ABSTRACT

A series of benchmark experiments were conducted at the CEA Valduc SILENE facility to create a new benchmark for the verification and validation of radiation transport codes and evaluated nuclear data used in the analysis of criticality accident alarm systems. The series consisted of three single-pulsed experiments with the SILENE reactor. The first experiment consisted of a bare reactor, while the second and third experiments used a lead and polyethylene

[1] V. Masse is presently at CEA/DEN/DADN/GIP

reflector, respectively. Several neutron activation foils and thermoluminescent dosimeters surrounded the reactor during each experiment, and some of these detectors had additional shielding materials between them and the reactor. This paper discusses a few recently uncovered details that impact the accuracy of the simulation of the first experiment. Additionally, the final benchmark data for the second and third experiments will be presented along with some preliminary computational results from simulations of the second and third experiments.

Key Words: SILENE, CAAS, Benchmark, Neutron Activation, TLD

1 INTRODUCTION

The United States Department of Energy (DOE) and the French Commissariat à l'Énergie Atomique et aux Énergies Alternatives (CEA) performed a series of benchmark experiments in 2010 intended for the verification and validation of radiation transport codes and evaluated nuclear data used in the analysis of criticality accident alarm systems (CAAS). Once evaluation of these experiments is complete, a full benchmark description will be published in the International Criticality Safety Benchmark Evaluation Project (ICSBEP) Handbook [1].

A description of the experimental details (source, detectors, and shielding materials) was published in reference 2, as well as some preliminary results of the neutron foil activities and Valduc thermoluminescent dosimeters (TLDs) for experiment 1 (bare reactor), the ORNL TLD measurement results for all three experiments, and preliminary computational results simulating the fast neutron activation foil responses for experiment 1 with SCALE 6.1 [3] and TRIPOLI-4®[2] [4]. Following that publication, additional information about the composition of materials used in the experiments has become available. In this paper, the preliminary measurement data provided in reference 2 for the bare reactor experiment is updated, and the final measurement values for experiments 2 and 3 are included. Lastly, some initial computational results simulating experiments 2 and 3 are presented. Note that reference 5 includes some updated simulation results for experiment 1 using SCALE 6.1 and details about part of the sensitivity and uncertainty analysis performed for the evaluation of experiment 1.

2 EXPERIMENTAL DETAILS

A detailed description of the experimental setup was published in reference 2. The following section provides a brief overview of the experiment setup, followed by a discussion of some new details that have been realized since its publication. These new details are important to the modeling and simulation of these experiments.

2.1 Experiment Overview

SILENE is a uranyl nitrate pulsed reactor with an annular geometry. During this series of experiments, SILENE was always operated with a single pulse. No reflector surrounded SILENE during the first experiment, but lead and polyethylene reflectors were used during the second and third experiments, respectively. During each experiment, the reactor was surrounded by a number of detectors including neutron activation foils, TLDs, CAAS detectors, and liquid scintillators. Some of these detectors had additional shielding materials between them and the bare or reflected reactor. These shielding materials included three different types of concrete

[2] TRIPOLI® is a registered trademark of CEA

shield blocks (which were provided by CEA Saclay): standard concrete, magnetite concrete, and barite concrete. Another shielding material, BoroBond™, which is a borated ceramic, was provided by Y-12. Figure 1 is a photograph of experiment 1 (bare reactor), and Table I provides a list of the neutron activation foils that were used in all the detector locations during the experiments along with the specific reaction products that were measured in each foil. In Section 4, computational results for the neutron activation foils and TLD inside Collimator A (see Figure 1) will be compared to the measured values reported in Section 3. Table II lists the number of fission events that occurred during experiments 2 and 3.

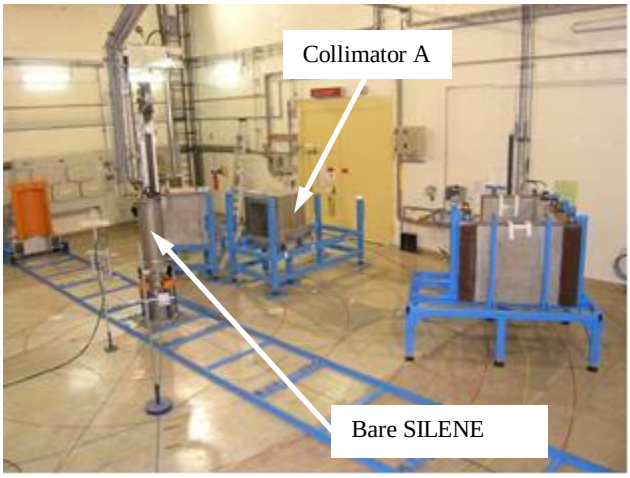

Figure 1. SILENE reactor cell experiment 1 configuration

Table I. Neutron activation foils

Foil	Reaction
Cobalt	$^{59}Co(n,\gamma)^{60}Co$
Gold	$^{197}Au(n,\gamma)^{198}Au$
Indium	$^{115}In(n,\gamma)^{116m}In$
Indium	$^{115}In(n,n'\gamma)^{115m}In$
Iron	$^{54}Fe(n,p)^{54}Mn$
Iron	$^{56}Fe(n,p)^{56}Mn$
Iron	$^{55}Mn(n,p)^{56}Mn$
Magnesium	$^{24}Mg(n,p)^{24}Na$
Nickel	$^{58}Ni(n,p)^{58}Co$

Table II. Reported number of fissions

Experiment 2	Experiment 3
2.14×10^{17}	1.92×10^{17}

2.2 New Experimental Details

In the preliminary comparison of experiment 1 [2], there is clearly poor agreement between the measured and calculated data inside Collimator B and for all the $^{56}Fe(n,p)^{56}Mn$ reactions. These differences led to further investigations that have uncovered some important facts pertinent to the computational model. The issues concerning the $^{56}Fe(n,p)^{56}Mn$ reactions in experiment 1 and corrections were previously reported [5], but the issue concerning agreement between calculations and measurement of the Collimator B foil activities was still being analyzed at the time of publication.

The difference in reference 2 between the measured and calculated results in experiment 1 Collimator B is due to the composition of the barite ($BaSO_4$) concrete shield between the detectors in Collimator B and the reactor. Dimensions and masses of the concrete shielding materials, which were used to accurately estimate the density of these materials and a chemical analysis of the various concrete materials, were previously discussed [6]. Unfortunately, the chemical analysis used to assay the barite concrete compositions did not assay Ba or S, which led to the large uncertainties associated with these elements. Use of “typical” Ba and S compositions in barite concrete [7] has produced much improved results compared to those reported previously [2]. However, further analysis is needed to determine if the measured data from Collimator B in experiment 1 is of significant quality to be included as part of the final benchmark evaluation.

Until that determination is final, no further comparisons between the experiment 1 Collimator B measured values and simulations will be published.

As reported previously [5], the difference between the measured and calculated results of the ^{56}Mn activity in the initial results [2] has been resolved. These initial simulations modeled the Fe foil as pure, natural occurring Fe. The final dosimetry reports provided by the CEA Valduc staff [8] included a chemical analysis of the neutron activation foils. As expected, each foil contained trace amounts of other elemental impurities. Since the trace ^{55}Mn impurity in the Fe foil (approximately 0.3 weight percent) serves as another path to produce ^{56}Mn, its inclusion will be very important to the final results. All subsequent simulations of this activation product include both production processes, ^{56}Fe(n,p)^{56}Mn and ^{55}Mn(n,γ)^{56}Mn.

The uncertainty on the number of fissions for each experiment was estimated at 5% [2], but Reference 9 provides a more accurate quantification of this uncertainty. When SILENE is bare, the uncertainty on the number of fissions is 4%, and 2% when surrounded by the lead reflector. No specific quantification of the uncertainty on the number of fissions is reported in reference 9 for SILENE surrounded by the polyethylene reflector, so it will be assumed this uncertainty is also 4%.

3 FINAL EXPERIMENTAL RESULTS

3.1 Experiment 1 Results

The measured data for experiment 1 presented in reference 2 were all labeled preliminary. These results have now been reviewed and are considered final (neutron activation foils and TLDs). However, there is one measurement in the experiment 1 data believed to be in error, which is the ^{198}Au activity in Collimator A. Unfortunately, the discrepancy was realized long enough after the experiment was complete that the ^{198}Au activity could not be reassessed due to the relatively short half-life. The possibility of an error was first realized after comparing the measured Collimator A ^{198}Au activity to a calculated estimate. In order to eliminate the possibility of any modeling errors, the assertion of this measurement error is justified by comparing all the ^{198}Au measurement data from this experiment.

Table III lists all the ^{198}Au activities measured in all three experiments where there was no shielding material between the gold foil and the reactor (bare or reflected). Below the reported activities in Table III is a set of ratios of these measured values (e.g., A/FF is the Collimator A activity divided by the Free Field activity). The distance between the foils in Collimator A and the Free Field location was identical within each individual experiment. The foils at Scattering Box locations 3 and 4 were always further away from the reactor than Collimator A and the Free Field location. Again, these foils had no additional shielding materials, other than the reactor reflectors, between themselves and the reactor. These foils did have different reflectors behind them, but these never changed during the different experiments.

Considering the facts about the shielding materials and distance from the reactor, the ratio A/FF should be about 1.0 or slightly greater than 1.0 due to the additional thermalization provided by the collimator box. The ratios A/SB3, A/SB4, FF/SB3, and FF/SB4 should be greater than 1.0 due to the differences in distance from the reactor (A and FF are closer). Finally, the ratios A/SB3 and FF/SB3 should be similar, and the same is true for A/SB4 and FF/SB4. The ratios A/FF, A/SB3, and A/SB4 for experiment 1 illustrate the measurement error for ^{198}Au in

Collimator A. The ratio A/FF for experiments 2 and 3 is about 1.0, but greater than 2.5 for experiment 1. The ratios A/SB3 and A/SB4 for experiment 1 are both greater than 4.0, but the same ratios for experiments 2 and 3 are all less than 2.0. Additionally, all the FF/SB3 and FF/SB4 ratios are less than 2.0. Based on these facts, it appears that the measured ^{198}Au activity in Collimator A for experiment 1 is high by about a factor of 2.5.

Table III. Comparison of Measured Gold Foil Results

Select Measured Dosimetry for Gold Activation Foil [Bq/gram]					
Experiment	Collimator A	Free Field		Scattering Box 3	Scattering Box 4
1	1.81×10^5	6.95×10^4		4.46×10^4	3.87×10^4
2	6.88×10^4	6.43×10^4		4.37×10^4	3.90×10^4
3	6.51×10^3	5.55×10^3		3.91×10^3	3.67×10^3
Comparisons of Measured Dosimetry					
Experiment	A/FF	A/SB3	A/SB4	FF/SB3	FF/SB4
1	2.60	4.06	4.68	1.56	1.80
2	1.07	1.57	1.76	1.47	1.65
3	1.17	1.66	1.77	1.42	1.51

3.2 Experiments 2 and 3 Results

The measurement data for experiments 2 and 3 have been verified and are ready for final publication. This data includes the activity of the neutron activation foils immediately following each experimental pulse and the absorbed dose of the various TLDs. The activity measurements are reported below in Table IV, and the measured TLD doses are reported in Table V. The coverage factor mentioned in Table V means the reported uncertainties are for the 95% confidence interval. In both of these tables a few values have been left out. These results were not reported because either the foil activity was too low to make a statistically accurate estimate of the activity immediately following the experimental pulse or the TLD absorbed dose was outside the reliable operating range for that specific TLD. One measurement that should be pointed out in Table IV is the ^{24}Na activity at the Scattering Box 1 location for experiment 2 (i.e., Mg foil). This activity was not reported in experiment 1 because of the activity being too low [2]. In experiment 2, a foil five times thicker was used in order to produce a larger activity, and the result is reported for experiment 2. However, the thicker Mg foil in experiment 3 did not provide enough ^{24}Na activity to produce a reliable measurement. None of the ^{54}Mn activities are provided in Table IV, which is primarily due to the small natural abundance of ^{54}Fe.

4 BENCHMARK EVALUATION

This series of experiments was conducted via a joint collaboration between the US DOE and the French CEA, and the benchmark evaluation will be a joint effort as well. Therefore, preliminary SCALE 6.1 and TRIPOLI-4® computational results are presented next. The final benchmark evaluation will also include MCNP [10] and COG [11] simulation results.

Table IV. Experiments 2 and 3 measured neutron foil activities

		Experiment 2		Experiment 3	
Position	**Reaction**	**Activity (Bq/g)**	**Relative Uncertainty (2 sigma)**	**Activity (Bq/g)**	**Relative Uncertainty (2 sigma)**
Collimator A	$^{59}Co(n,\gamma)^{60}Co$	6.090×10^{1}	4.3%	4.550×10^{0}	4.4%
	$^{197}Au(n,\gamma)^{198}Au$	6.880×10^{4}	3.1%	6.510×10^{3}	6.0%
	$^{115}In(n,\gamma)^{116m}In$	7.950×10^{6}	4.2%	6.680×10^{5}	3.4%
	$^{115}In(n,n'\gamma)^{115m}In$	6.100×10^{3}	3.4%	9.930×10^{2}	3.1%
	$^{54}Fe(n,p)^{54}Mn$	---	---	---	---
	$^{56}Fe(n,p)^{56}Mn$	2.020×10^{3}	5.0%	1.879×10^{2}	3.1%
	$^{24}Mg(n,p)^{24}Na$	2.480×10^{1}	4.0%	1.620×10^{1}	8.6%
	$^{58}Ni(n,p)^{58}Co$	6.860×10^{0}	3.2%	2.153×10^{0}	3.2%
Collimator B	$^{59}Co(n,\gamma)^{60}Co$	3.230×10^{1}	4.3%	6.600×10^{-1}	2.3%
	$^{197}Au(n,\gamma)^{198}Au$	3.101×10^{4}	3.1%	1.171×10^{3}	3.1%
	$^{115}In(n,\gamma)^{116m}In$	3.840×10^{6}	3.9%	1.098×10^{5}	4.6%
	$^{115}In(n,n'\gamma)^{115m}In$	9.400×10^{2}	3.9%	4.110×10^{2}	3.2%
	$^{54}Fe(n,p)^{54}Mn$	---	---	---	---
	$^{56}Fe(n,p)^{56}Mn$	1.040×10^{3}	2.9%	4.160×10^{1}	3.6%
	$^{24}Mg(n,p)^{24}Na$	5.520×10^{0}	11.2%	7.690×10^{0}	6.2%
	$^{58}Ni(n,p)^{58}Co$	1.271×10^{0}	3.2%	---	---
Free Field Location	$^{59}Co(n,\gamma)^{60}Co$	6.270×10^{1}	4.5%	5.000×10^{0}	4.4%
	$^{197}Au(n,\gamma)^{198}Au$	6.430×10^{4}	3.1%	5.550×10^{3}	3.2%
	$^{115}In(n,\gamma)^{116m}In$	7.850×10^{6}	3.8%	5.870×10^{5}	4.4%
	$^{115}In(n,n'\gamma)^{115m}In$	5.210×10^{3}	3.5%	8.410×10^{2}	6.2%
	$^{54}Fe(n,p)^{54}Mn$	---	---	---	---
	$^{56}Fe(n,p)^{56}Mn$	2.084×10^{3}	2.5%	2.140×10^{2}	5.6%
	$^{24}Mg(n,p)^{24}Na$	2.640×10^{1}	7.2%	1.470×10^{1}	8.2%
	$^{58}Ni(n,p)^{58}Co$	6.340×10^{0}	3.2%	1.794×10^{0}	3.2%
Scattering Box 1	$^{59}Co(n,\gamma)^{60}Co$	2.440×10^{1}	4.5%	2.167×10^{0}	4.4%
	$^{197}Au(n,\gamma)^{198}Au$	2.412×10^{4}	3.1%	2.360×10^{3}	6.4%
	$^{115}In(n,\gamma)^{116m}In$	2.910×10^{6}	4.5%	2.650×10^{5}	3.8%
	$^{115}In(n,n'\gamma)^{115m}In$	3.230×10^{2}	3.4%	5.880×10^{1}	3.7%
	$^{54}Fe(n,p)^{54}Mn$	---	---	---	---
	$^{56}Fe(n,p)^{56}Mn$	8.810×10^{2}	2.5%	7.830×10^{1}	3.3%
	$^{24}Mg(n,p)^{24}Na$	1.206×10^{0}	6.3%	---	---
	$^{58}Ni(n,p)^{58}Co$	3.230×10^{-1}	4.0%	---	---
Scattering Box 2	$^{59}Co(n,\gamma)^{60}Co$	2.810×10^{1}	4.3%	2.517×10^{0}	2.4%
	$^{197}Au(n,\gamma)^{198}Au$	2.583×10^{4}	3.0%	2.509×10^{3}	3.0%
	$^{58}Ni(n,p)^{58}Co$	1.898×10^{-1}	3.3%	---	---
Scattering Box 3	$^{59}Co(n,\gamma)^{60}Co$	4.570×10^{1}	4.2%	3.910×10^{0}	4.3%
	$^{197}Au(n,\gamma)^{198}Au$	4.370×10^{4}	3.2%	3.910×10^{3}	3.1%
	$^{58}Ni(n,p)^{58}Co$	1.750×10^{0}	6.3%	---	---
Scattering Box 4	$^{59}Co(n,\gamma)^{60}Co$	4.120×10^{1}	4.4%	3.471×10^{0}	2.3%
	$^{197}Au(n,\gamma)^{198}Au$	3.900×10^{4}	3.3%	3.670×10^{3}	6.0%
	$^{58}Ni(n,p)^{58}Co$	1.830×10^{0}	6.6%	---	---

Table V. Experiments 2 and 3 measured TLD absorbed doses (Gy) and relative uncertainties (coverage factor k=2)

		Experiment 2		Experiment 3	
Position	**TLD**	**Dose**	**Rel Unc**	**Dose**	**Rel Unc**
Collimator A	Al_2O_3	0.820	4.8%	5.29	4.5%
	HBG	1.06	6.0%	5.38	6.0%
	DXT	1.02	6.0%	7.13	6.0%
Collimator B	Al_2O_3	0.550	2.0%	3.15	10.2%
	HBG	0.620	6.0%	3.17	6.0%
	DXT	0.573	6.0%	3.53	6.0%
Free Field Location	Al_2O_3	0.562	5.2%	4.79	13.8%
	HBG	0.760	6.0%	4.83	6.0%
	DXT	0.589	6.0%	5.60	6.0%
Scattering Box 1	Al_2O_3	---	---	---	---
	HBG	0.402	6.0%	0.202	6.0%
	DXT	0.371	6.0%	0.184	6.0%
Scattering Box 2	Al_2O_3	---	---	---	---
	HBG	0.350	6.0%	0.115	6.0%
	DXT	0.294	6.0%	0.149	6.0%
Scattering Box 3	Al_2O_3	0.420	7.1%	1.01	11.9%
Scattering Box 4	Al_2O_3	0.780	4.5%	1.14	6.8%
External cell table	HBG	1.1×10^{-4}	40%	1×10^{-5}	150%
	DXT	5×10^{-5}	60%	---	---
External cell wall	HBG	5×10^{-5}	60%	2×10^{-5}	100%
	DXT	2×10^{-5}	100%	---	---

4.1 SCALE Evaluation

These experiments are modeled with the CAAS modeling capability [12] of the MAVRIC [3] sequence in SCALE 6.1. This requires that the experiments be modeled in two steps. The first step is to calculate the spatial and energy-dependent distribution of fission neutrons for each critical configuration of SILENE, which is done using the KENO-VI [3] eigenvalue code with multi-group cross sections. In the second step, these distributions of fission neutrons are used as sources by the MAVRIC sequence to calculate the response of the detectors in the experiments.

The multi-group cross sections used in these calculations have 200 neutron groups and 47 photon groups and are based on ENDF/B-VII.0. This cross-section library is a standard transport library available with distributions of SCALE 6.1. These cross sections also provide the detector response functions to calculate the foil activities. One exception to this is the $^{115}In(n,n'\gamma)^{115m}In$ reaction. The response function for the inelastic scattering reaction in indium is taken from the 2002 version of the International Reactor Dosimetry File [13]. The response function used to calculate the TLD response is the International Commission on Radiation Units and Measurements (ICRU) air kerma flux-to-dose conversion factors [14], which are also available in SCALE.

4.2 TRIPOLI-4® Evaluation

The continuous energy TRIPOLI-4® [4] Monte Carlo transport code has been extensively applied on criticality safety, radiation shielding, and reactor physics calculations [15-17]. In this benchmark, different calculation modes of the code were performed to analyze the experiments.

The combinatorial geometry option [16] and T4G display tool [18] were first applied to model the SILENE reactor, lead and polyethylene annuli shielding wall around the outside of the SILENE core, multi-layer collimators, concrete shields, scattering box, and fission neutron source measurement facilities. The experimental concrete room was also modeled so as to consider the room scattering effect in these calculations. Both the CEA-V5 nuclear data library based on JEFF-3.1.1 [19] evaluation and the 2002 version of the International Reactor Dosimetry File were used in this study for neutron transport and detector response calculations.

Under the criticality mode of TRIPOLI-4® fission neutron source distributions were initially calculated for pulses 2 and 3 with the standard flux tally. Using the calculated neutron source distribution and the measured fission neutron intensity, a parallel shielding mode TRIPOLI-4® calculation was applied to calculate the detector responses of the fast neutron activation foils, ^{58}Ni(n,p), ^{54}Fe(n,p), ^{115}In(n,n'), ^{24}Mg(n,p) and ^{56}Fe(n,p).

A separate shielding mode model was developed to calculate the slow neutron detector responses, ^{115}In(n,γ), ^{59}Co(n, γ), ^{197}Au(n, γ), and ^{55}Mn(n, γ). All detectors were exactly introduced into this slow neutron calculation model so as to properly consider the self-shielding effect of the detectors in the TRIPOLI-4® full energy run (20 MeV – 1E-11 MeV).

A coupled neutron-gamma model was also prepared to calculate the TLD dosimetry experiments with variance reduction options. These options are helpful to improve the secondary gamma-ray production in calculations and the uncertainty of calculated TLD results. The response functions used to calculate the TLD response are the ICRU-57 air kerma flux-to-dose conversion factors, which were also applied in TRIPOLI-4®.

4.3 Computational Results: Collimator A Measurements for Experiments 2 and 3

Preliminary SCALE 6.1 and TRIPOLI-4® simulation results for the Collimator A measurements in experiments 2 and 3 are presented in Table VI. Comparisons between the Collimator A measurements and calculations are presented as ratios of the calculated results to the experimental results (C/E), so perfect agreement is represented by a ratio of 1.0 with a relative uncertainty of 0%. The computational uncertainties of the SCALE 6.1 experiment 2 calculations are all less than 1%, except for the ^{56}Mn activity and the TLD dose, which are both a little more than 1.5%. The SCALE 6.1 computational uncertainties of the experiment 3 simulations of threshold reactions (n,p reactions) are all less than 1%, and the uncertainties for the thermal reactions (n,γ reactions) and the TLD dose are between 1.5% and 2.5%. The computational uncertainties of the TRIPOLI-4® experiment 2 calculations are less than 1.5% for the threshold reactions and less than 4% for the thermal reactions and TLD dose. Finally, the computational uncertainties of the TRIPOLI-4® experiment 3 calculations are less than 2.1% for the threshold reactions and less than 6% for the thermal reactions and TLD dose. Note that the production of the ^{56}Mn activation product is nearly entirely dominated by the thermal reaction. The computational uncertainties along with the measurement uncertainties have been used to calculate the uncertainties of the C/E ratios in Table VI.

Table VI. Comparison of computational and measured results for simulations of Collimator A

		SCALE 6.1		TRIPOLI-4®	
Position	**Reaction**	**Ratio: C/E**	**Relative Uncertainty (2 sigma)**	**Ratio: C/E**	**Relative Uncertainty (2 sigma)**
Experiment 2 Collimator A	$^{59}Co(n,\gamma)^{60}Co$	1.16	4.62%	1.04	5.40%
	$^{197}Au(n,\gamma)^{198}Au$	1.21	3.59%	1.18	8.47%
	$^{115}In(n,\gamma)^{116m}In$	1.50	4.58%	1.11	7.63%
	$^{115}In(n,n'\gamma)^{115m}In$	0.94	3.75%	0.93	4.44%
	$^{56}Fe(n,p)^{56}Mn$ + $^{55}Mn(n,\gamma)^{56}Mn$	1.14	6.01%	0.91	7.93%
	$^{24}Mg(n,p)^{24}Na$	1.20	4.30%	1.08	4.42%
	$^{58}Ni(n,p)^{58}Co$	1.08	3.39%	1.09	3.31%
	TLD - Al_2O_3	0.79	5.81%	0.69	7.82%
Experiment 3 Collimator A	$^{59}Co(n,\gamma)^{60}Co$	0.95	5.50%	0.93	7.04%
	$^{197}Au(n,\gamma)^{198}Au$	0.87	7.93%	0.89	13.4%
	$^{115}In(n,\gamma)^{116m}In$	1.14	5.97%	0.89	7.53%
	$^{115}In(n,n'\gamma)^{115m}In$	0.83	3.58%	0.96	4.40%
	$^{56}Fe(n,p)^{56}Mn$ + $^{55}Mn(n,\gamma)^{56}Mn$	0.86	4.47%	0.92	5.43%
	$^{24}Mg(n,p)^{24}Na$	1.00	8.82%	0.90	8.87%
	$^{58}Ni(n,p)^{58}Co$	0.90	3.55%	0.95	5.28%
	TLD - Al_2O_3	0.62	5.53%	0.71	5.62%

The uncertainty on the number of fissions discussed at the end of section 2.2 was not accounted for in Table VI, even though all the simulations were normalized to the reported number of fissions listed in Table II. Below in Figures 2 and 3 are plots of the C/E ratios in Table VI with error bars that include the Monte Carlo uncertainty of the calculations, the uncertainty on the number of fission events, and the uncertainty of the experimentally measured values. Figures 2 and 3 plot the ratios for experiments 2 and 3, respectively.

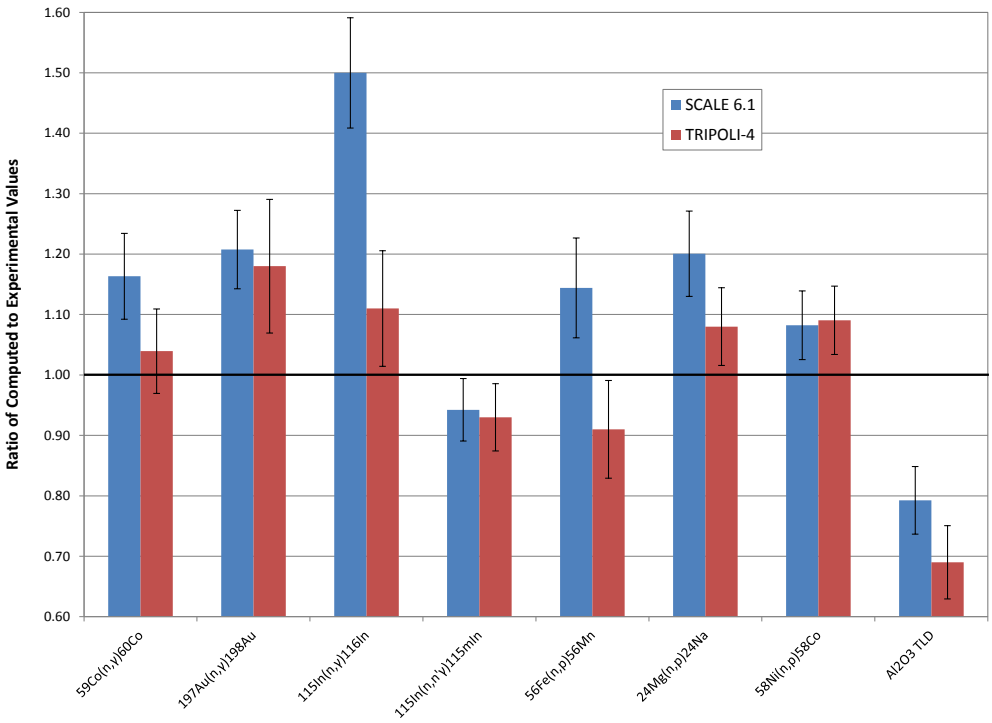

Figure 2. C/E ratios for experiment 2 including number of fission events uncertainty (error bars 2 sigma)

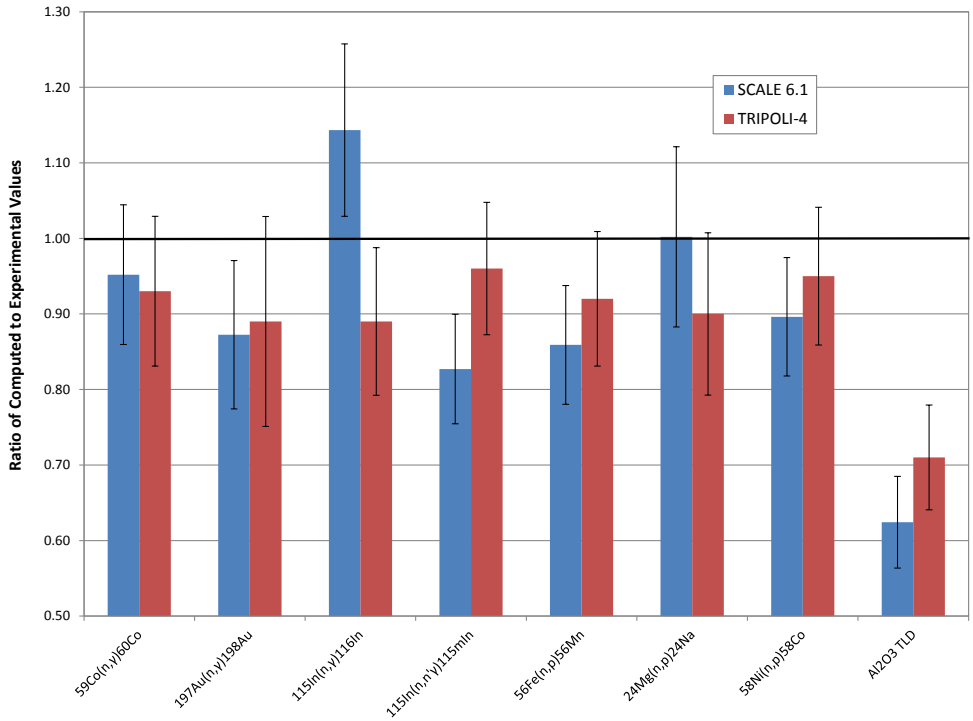

Figure 3. C/E ratios for experiment 3 including number of fission events uncertainty (error bars 2 sigma)

5 SUMMARY AND CONCLUSIONS

The final measurement data of the 2010 SILENE CAAS benchmark experiments 2 and 3 have been presented along with preliminary SCALE 6.1 and TRIPOLI-4® simulations of the Collimator A detector responses. The measurement data for experiment 1, published in reference 2, has been reviewed and is now final. However, it has been determined that the experiment 1 measurement of ^{198}Au activity in Collimator A was erroneous.

The SCALE simulations of experiment 2 using response cross sections based on ENDF/B-VII.0 tend to over predict the experiment. The IRDF-2002 response cross section for ^{115m}In under predicts the measurement as does the ICRU air kerma response function used for the TLD.

The SCALE simulations of experiment 3 using response cross sections based on ENDF/B-VII.0 and IRDF-2002 tend to under predict the experiment, the one exception being the ENDF response cross section for ^{116}In, which over predicts the measurement. Again, the ICRU air kerma response function used for the TLD under predicts the experiment, but the under prediction appears worse for experiment 3 than for experiment 2.

The TRIPOLI-4® results are statistically the same as the SCALE results and follow the same trend of over prediction or under prediction as SCALE except for a few cases. For experiment 2 the TRIPOLI-4® results of the ^{115}In(n,γ)^{116}In and ^{56}Fe(n,p)^{56}Mn reactions are statistically different from the SCALE results, and the same is true for the ^{115}In(n,γ)^{116}In reaction in experiment 3. The TRIPOLI-4® results for these three reactions are in better agreement with the experiment than the SCALE results. Since the thermal indium reaction disagrees between both of the experiments that might suggest a potential problem with the SCALE multi-group representation of the ^{115}In capture cross section. Plus, the SCALE thermal indium reaction is a clear outlier when comparing all the SCALE results for experiment 2 or 3. Similarly, the TRIPOLI-4® Mn production in experiment 2 does not follow the trend of the calculations over predicting the experiment. Since the agreement for Mn production in experiment 3 is in agreement between the two codes and because the Mn production is based on the sum of two reactions, it is not possible to surmise what might be causing the difference without a more detailed evaluation of the results.

Overall the computational values agree with the experimentally measured values moderately well, considering that biases and uncertainties for shielding benchmarks are normally much larger than those for critical benchmarks. Biases and uncertainties in the range of 10 to 20 percent are typical, and this has been achieved so far for this benchmark.

At this point there are several things that must be finalized before the benchmark can be presented to the ICSBEP. Simulations of the remaining aspects of experiments 2 and 3 must be completed. Use of another response function for the TLD simulations should be considered, particularly an Al_2O_3 kerma response function. Further evaluation of the simulation results for reactions ^{115}In(n,γ)^{116}In and ^{56}Fe(n,p)^{56}Mn. Lastly, an uncertainty analysis, like that in reference 5, must be completed for all aspects of each experiment. Once approved and published by the ICSBEP, these experiments will serve as a useful tool for verifying and validating radiation transport codes and nuclear data used for the evaluation of CAAS.

6 ACKNOWLEDGMENTS

The work documented in this paper was performed with support from the US Department of Energy Nuclear Criticality Safety Program.

The CEA Saclay authors gratefully acknowledge EDF and AREVA for their support of TRIPOLI-4®.

This manuscript has been authored by the Oak Ridge National Laboratory, managed by UT-Battelle LLC under Contract No. DE-AC05-00OR22725 with the US Department of Energy. The US Government retains and the publisher, by accepting the article for publication, acknowledges that the US Government retains a nonexclusive, paid-up, irrevocable, worldwide license to publish or reproduce the published form of this manuscript, or allow others to do so, for US Government purposes.

7 REFERENCES

1. "International Handbook of Evaluated Criticality Safety Benchmark Experiments," NEA/NSC/DOC(95)03, Organization for Economic Co-operation and Development – Nuclear Energy Agency (OECD-NEA), September 2012 Edition.
2. T. M. Miller, et. al., "2010 Criticality Accident Alarm System Benchmark Experiments at the CEA Valduc SILENE Facility," *International Conference on Nuclear Criticality 2011*, Edinburgh, Scotland, September 19-22, 2011, on CD-ROM (2011).
3. SCALE Development Team, "SCALE: A Comprehensive Modeling and Simulation Suite for Nuclear Safety Analysis and Design," ORNL/TM-2005/39, Version 6.1, Oak Ridge National Laboratory (June 2011).
4. TRIPOLI-4® Project Team, "TRIPOLI-4® Version 4 User Guide," CEA-R-6169, Commissariat à l'Énergie Atomique et aux Énergies Alternatives (2008).
5. K. H. Reynolds, T. M. Miller, and L. F. Miller, "Sensitivity and Uncertainty Analysis of a Fixed Source Criticality Accident Alarm System Benchmark Experiment," *2013 Topical Meeting on Nuclear Criticality Safety*, Wilmington, North Carolina, September 29 – October 3, 2013, on CD-ROM (2013).
6. J. Piot, "2010 CAAS Test on the SILENE Reactor, Data for CAAS Experiment Modeling," CEA/VA/DRMN/SRNC DO 428, Commissariat à l'Énergie Atomique et aux Énergies Alternatives (2011).
7. "ANSI/ANS-6.4-2006 Nuclear Analysis and Design of Concrete Radiation Shielding for Nuclear Power Plants," American Nuclear Society, La Grange Park, IL (2006).
8. X. Jacquet, G. Rousseau, and L. Savanier, "Rapport d'Essais – Dossier d'Experience N°2011/014.a", "Rapport d'Essais – Dossier d'Experience N°2011/015.a", "Rapport d'Essais – Dossier d'Experience N°2011/016.a", Commissariat à l'Énergie Atomique et aux Énergies Alternatives (2011, 2012, and 2012).

9. K. Hamon, "Calibration of SILENE Reactor," Commissariat à l'Énergie Atomique - Centre d'etudes de Valduc, Department de recherche en Neutronique et Criticite, CEA Valduc (2004).

10. X-5 Monte Carlo Team, "MCNP—A General Monte Carlo N-Particle Transport Code, Version 5," LA-UR-03-1987, Los Alamos National Laboratory (Revised 2008).

11. S. Kim, D. Heinrichs, R. Buck, E. Lent, and C. Lee, "COG Preliminary Results for a SILENE Criticality Excursion Benchmark Experiment," *Transactions of the American Nuclear Society*, **108**, p. 463 (2013).

12. T. M. Miller and D. E. Peplow, "Corrected User Guidance to Perform Three-Dimensional Criticality Accident Alarm System Modeling with SCALE," *Transactions of the American Nuclear Society*, **108**, p. 498 (2013).

13. O. Bersillon, et. al., "International Reactor Dosimetry File – 2002 (IRDF – 2002)," STI/DOC/010/452, International Atomic Energy Agency (2006).

14. ICRU-57, "Conversion Coefficients for Use in Radiological Protection Against External Radiation," International Commission on Radiation Units and Measurements, Bethesda, MD (1998).

15. Y. K. Lee, et. al., "CRISTAL Criticality Safety Package Validation: TRIPOLI-4® Monte Carlo Code, JEF2.2 Library and ICSBEP Experiments," *Sixth Int. Conf. on Nuclear Criticality Safety*, Versailles, France, September 20–24, 1999.

16. Y. K. Lee, "Analysis of the LEU-COMP-THERM-049 Maracas Critical Configurations Using TRIPOLI-4.3® 3D Lattices Geometry and JEFF-3.0 Library," *Seventh International Conference on Nuclear Criticality Safety*, Tokai, Japan, October 20-24, 2003, p. 114 (2003).

17. Y. K. Lee, F. X. Hugot, "TRIPOLI-4®: Verification and Validation," *J. Trans. Am. Nucl. Soc.* **97**, p. 523 (2007).

18. F. X. Hugot, Y. K. Lee, "A New Prototype Display Tool for the Monte Carlo Particle Transport Code TRIPOLI-4®," *Progress in Nuclear Science and Technology (SNA+MC 2010)*, **2**, p. 851 (2011).

19. A. Santamarina, D. Bernard, et. al., "The JEFF-3.1.1 Nuclear Data Library," JEFF Report 22, Organisation for Economic Co-operation and Development / Nuclear Energy Agency (2009).